

Location and energy of interstitial hydrogen in the 1/1 approximant W -TiZrNi of the icosahedral TiZrNi quasicrystal: Rietveld refinement of x-ray and neutron diffraction data and density-functional calculations

R. G. Hennig,^{1,2} E. H. Majzoub,^{3,2} and K. F. Kelton²

¹*Department of Physics, Ohio State University, Columbus, Ohio 43210, U.S.A.*

²*Department of Physics, Washington University, St. Louis, Missouri 63130, U.S.A.*

³*Sandia National Laboratories, Livermore, California 94550, U.S.A.*

(Received 11 February 2006; published 25 May 2006)

We present a determination of hydrogen sites in the 1/1 approximant structure of the icosahedral TiZrNi quasicrystal. A Rietveld refinement of neutron and x-ray diffraction data determines the locations of interstitial hydrogen atoms. Density-functional methods calculate the energy of hydrogen on all possible interstitial sites. The Rietveld refinement shows that the hydrogen atoms are preferentially located in the two lowest-energy sites. The filling of the remaining hydrogen sites is dominated by the repulsive hydrogen-hydrogen interaction at short distances.

DOI: [10.1103/PhysRevB.73.184205](https://doi.org/10.1103/PhysRevB.73.184205)

PACS number(s): 61.44.Br, 61.72.Dd, 61.12.Ld, 71.15.Mb

I. INTRODUCTION

Hydrogen absorption in materials is technologically important for hydrogen storage applications and scientifically interesting as a local structural probe for complex materials. Ti–Zr–Ni alloys absorb large amounts of hydrogen^{1–5} and display a variety of complex intermetallic structures.^{6–9} Specifically, the icosahedral TiZrNi quasicrystal and its approximant structure, W -TiZrNi, absorb hydrogen up to a concentration of 1.8 hydrogen atoms per metal atom at pressures up to 100 kPa.^{1–3} The sloping pressure plateau¹ makes them less suitable for hydrogen storage applications at low pressures compared to traditional AB₂ and AB₅ hydrogen storage alloys,¹⁰ however, recent work revealed a possible high-pressure plateau at about 2 MPa that might lead to useful applications.¹ The hydrogen absorption in quasicrystals also opens the exciting possibility of using hydrogen as a structural probe in x-ray spectroscopy¹¹ and NMR (Ref. 12) experiments to investigate local order in the quasicrystal and the approximant phase. Here we present the determination of the hydrogen sites in the known W -TiZrNi structure, a necessary first step toward validating hydrogen as a local probe.

The extraction of structural information from experimental measurements of hydrogen in materials has proven to be difficult and requires theoretical modeling of the structure and the energetics of the hydrogen absorption process. For example, NMR second moment measurements¹² of the icosahedral TiZrNi quasicrystal remain inconclusive, despite using an accurate structural model of the icosahedral TiZrNi quasicrystal.^{8,9}

Another approach for extracting structural information from hydrogen in metals is based on hydrogen absorption experiments, where the chemical potential of hydrogen can be measured as a function of the hydrogen concentration. From the chemical potential, information about the hydrogen site energies can be extracted. This approach has been applied to a number of amorphous alloys.^{13–17} The pressure dependence of the absorption of hydrogen has been measured for the W phase and the quasicrystal.^{4,18} Understanding of the energetics of the hydrogen absorption requires knowl-

edge of the hydrogen site energy distribution.

The absorption of hydrogen and the filling of the available hydrogen sites is strongly affected by the interaction between the hydrogen atoms. Switendick observed from a compilation of experimental data that the minimum distance between hydrogen atoms in ordered metal hydrides is larger than 2 Å.¹⁹ This empirical rule was later supported by band-structure calculations,²⁰ which ascribe the effect to repulsive interactions generated by the screening cloud of the hydrogen atoms.

In this work we determine the location and energy of hydrogen in the W -TiZrNi phase using diffraction data and density-functional calculations. The filling of the resulting site energy distribution provides insight into the repulsive interaction of hydrogen at short distances. Section II describes the structure of the W -TiZrNi phase. In Sec. III the location of the hydrogen atoms are refined by a Rietveld refinement of neutron and x-ray diffraction data. The hydrogen site energy distribution is determined by density-functional calculations in Sec. IV. The experimental occupations of the hydrogen sites combined with the site energies provide insight into the hydrogen interactions. In Sec. V we discuss the hydrogen-metal and hydrogen-hydrogen interactions and find a closest distance between hydrogen atoms of about 2 Å and a repulsive interaction of about 0.2 to 0.4 eV in good agreement with the work by Switendick.¹⁹

II. STRUCTURE OF W -TiZrNi

The W -TiZrNi phase is a periodic crystalline phase closely related to the icosahedral quasicrystal.⁸ The structure of the W phase was determined using x-ray diffraction and neutron scattering data and confirmed by *ab initio* calculations.^{7,21} It consists of a body centered cubic packing of icosahedral Bergman clusters connected by a few “glue” sites. The Bergman cluster, as shown in Fig. 1, is composed of a central Ni atom surrounded by a small icosahedron of 12 Ti atoms. A second icosahedron is formed by placing 12 Ni atoms directly outside the vertices of the small icosahedron.

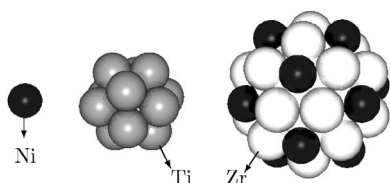


FIG. 1. Structure of the Bergman cluster consisting of a central Ni atom (left), a small icosahedron of Ti atoms (center), and a large icosahedron of Ni atoms with Zr atoms on the face centers (right).

Finally 20 Zr atoms are placed on the faces of the large icosahedron. The remaining 36 “glue” sites consist of 24 Ti atoms, forming a hexagon that separates the Bergman clusters along the threefold $\langle 111 \rangle$ directions, and 12 Ti and Zr atoms, forming a rhombus that divides the Bergman clusters along the twofold $\langle 100 \rangle$ directions.

The structure of the W -TiZrNi approximant is closely related to the i -TiZrNi quasicrystal; for both, the Bergman cluster presents the main structural motif. The structure of the quasicrystal was modeled by a canonical cell tiling²² that maximizes the volume fraction of Bergman cluster. The atomic decoration of this random tiling was refined by x-ray and neutron diffraction data and density-functional calculations.^{8,9} Since the canonical cell tiling is a random tiling model, a higher dimensional representation of the atomic structure by a simple acceptance domain is unknown.

III. HYDROGEN SITES FROM DIFFRACTION

A. Sample preparation and data acquisition

Raw materials were purchased from Alpha Aesar with oxygen concentrations of 166, 70, and 66 ppm for Ti, Zr, and Ni, respectively. Alloy ingots of composition $\text{Ti}_{50}\text{Zr}_{35}\text{Ni}_{15}$ were prepared in an arc furnace with a water-cooled Cu hearth, in a high-purity Ar gas atmosphere. The ingots were annealed under 1/3 atm 99.99% pure Ar for approximately five days at 600 °C in fused silica tubes, which contained a Ti getter at one end. Prior to annealing, the Ti getter was heated alone using a rf coil to further reduce any residual oxygen in the quartz tube. The ingots were deuterated to a H/M of 0.30 through gas-phase loading. Prior to hydrogen exposure, the samples were etched in an Ar plasma, and vapor deposited with Pd. The Pd coating both dissociates molecular hydrogen and prevents passivation of the sample surface. Hydrogenated ingots were ground into a powder for subsequent analysis.

Neutron powder diffraction data were obtained at the University of Missouri Research Reactor (MURR) using a bent Si monochromator. The neutron wavelength was 1.4875 Å. The data were collected using a 20° 2θ linear position sensitive detector and binned into 0.05° steps. Each 20° section of data was collected up to a monitor count of $25 \cdot 10^6$. The sample was contained inside a thin-walled cylindrical vanadium canister with a diameter of 3 mm.

Powder x-ray diffraction was performed on a Rigaku *Geigerflex* in the Bragg-Brentano geometry using Cu K_α radiation and a graphite exit monochromator, with a count time of 1 sec per step size of 0.05° 2θ .

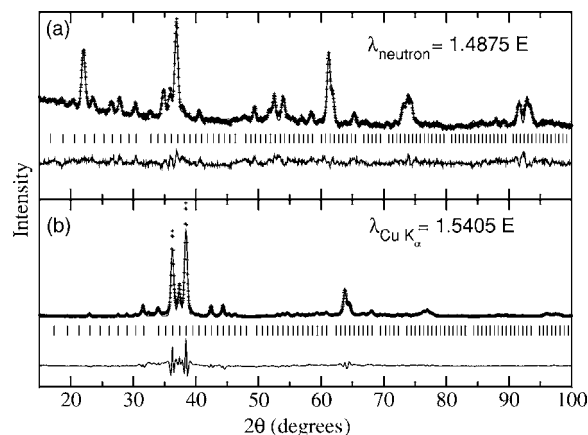


FIG. 2. Rietveld refinement of deuterated W -phase (a) neutron, and (b) x-ray data. The measured data are indicated by “+” and the solid line denotes the fit. The difference curve is shown in the bottom of each panel. Vertical bars represent Bragg reflection positions.

Rietveld refinement

A Rietveld refinement of the neutron and x-ray powder diffraction data was performed to determine the hydrogen locations in the interstitial sites of the crystal approximant using the general structural analysis system (GSAS).²³ Refinement results for the W phase are shown in Fig. 2 and Table I. Previously determined atomic coordinates of Ti, Zr, and Ni atoms in the $W(1/1)$ structure were used as a starting configuration.⁷ Candidate deuterium positions were determined from the $W(1/1)$ structure by finding all available tetrahedral interstitial sites. The metal atom locations were not refined while adding deuterium atoms to the interstitial locations, which were added successively to each available Wyckoff site and refined for position, as allowed by symmetry, and occupation number. Only sites resulting in a refined occupation of greater than 1% are shown in Table I. Following the addition of deuterium atoms, the metal atoms were again refined for position. The lattice parameter, and the isotropic Debye-Waller factors for the deuterium atoms were also allowed to vary. The lattice parameter increases from a deuterium-free fit of 14.30 to 14.42 Å. The quality of the structural analysis is reflected by the residual, $R_p=2.8\%$, and the weighted residual, $R_{wp}=4.5\%$, as well as the “goodness of fit” $\chi^2=0.76$. Definitions of the residuals can be found in the GSAS technical manual.²³ The chemistry of the fit results in a H/M of 0.32, in close agreement with the experimental value of 0.30.

Table I shows the results of the Rietveld refinement for the deuterated W -TiZrNi phase. About 90% of the deuterium atoms are located in the three sites H_1 , H_2 , and H_{13} . In the following section density-functional calculations determine the site energies of hydrogen in the W -TiZrNi phase. The results show that the two highest occupied sites H_1 and H_2 correspond to the lowest-energy sites.

IV. DENSITY-FUNCTIONAL CALCULATIONS OF HYDROGEN SITE ENERGIES

Density-functional calculations determine the hydrogen site energies. The density-functional total energy calculations

TABLE I. Hydrogen H_i and metal atom M_i positions and site occupations from the Rietveld refinement of deuterated W -phase $\text{Ti}_{50}\text{Zr}_{35}\text{Ni}_{15}$. The refined value for H/M is 0.32, in close agreement with the experimental value of 0.30. For simplicity we denote the hydrogen sites of the Rietveld refinement with the same label as the corresponding site of the site energy distribution in Table II.

cI162		Space group $Im\bar{3}$			$a_0=14.418 \text{ \AA}$
$R_{wp}=4.4\%$,		$R_p=2.7\%$,			$\chi^2=0.73$
	Site	x	y	z	Occupancy
M_1	2(a)	0.000	0.000	0.000	Ni(1.0)
M_2	24(g)	0.000	0.103	0.161	Ti(1.0)
M_3	24(g)	0.000	0.189	0.306	Ni(1.0)
M_4	16(f)	0.187	0.187	0.187	Zr(1.0)
M_5	24(g)	0.000	0.309	0.112	Zr(1.0)
M_6	12(e)	0.197	0.000	0.500	Zr(0.61)/Ti(0.39)
M_7	48(h)	0.146	0.189	0.400	Zr(0.13)/Ti(0.87)
M_8	12(e)	0.416	0.000	0.500	Ti(0.57)/Ni(0.43)
H_1	12(d)	0.000	0.000	0.391	D(0.81)
H_2	48(h)	0.107	0.314	0.186	D(0.68)
H_{13}	24(g)	0.000	0.430	0.310	D(0.13)
H_9	48(h)	0.110	0.140	0.300	D(0.06)
H_{19}	48(h)	0.030	0.200	0.420	D(0.05)
H_{10}	48(h)	0.070	0.390	0.190	D(0.01)
H_6	12(d)	0.000	0.000	0.240	D(0.01)
H_4	48(h)	0.110	0.070	0.430	D(0.01)

were performed with VASP,^{24,25} a density-functional code using a plane-wave basis and ultrasoft Vanderbilt type pseudopotentials.^{26,27} The generalized gradient approximation by Perdew and Wang was used.²⁸ A plane-wave kinetic-energy cutoff of 302 eV ensured convergence of the energy to 1 meV/atom. The calculations were performed at the Γ -point resulting in an accuracy of the relative hydrogen site energies of about 10 meV.

The possible hydrogen sites are given by the interstitial tetrahedra of the W phase. For each individual site, the hydrogen site energy was calculated by placing a single hydrogen atom at the center of each inequivalent tetrahedron in the relaxed structure of the W phase. The position of the hydrogen atom is relaxed until the atomic-level forces are smaller than 20 meV/ \AA , while keeping the metal atoms fixed and the shape and size of the unit cell constant. The hydrogen site energies were measured relative to the density-functional energy of molecular hydrogen. Table II lists the resulting hydrogen site energies and positions.

Figure 3 displays the hydrogen site energy distribution. The total width of the distribution is about 700 meV. The energy distribution consists of a set of low-energy sites with energies around -800 meV, a large number of sites with energies ranging from -700 to -450 meV and a tail of high energy sites. The three lowest-energy sites H_1 – H_3 of the distribution are separated by a gap of about 100 meV from the main distribution.

The energy of a hydrogen site depends strongly on both the chemistry of the neighboring metal atoms and the geometry of the interstitial site. All low-energy sites with $E < -630$ meV are located in the “glue” region between the

Bergman clusters in tetrahedra with the stoichiometry of Ti_2Zr_2 and Ti_3Zr . In contrast the high-energy sites with $E > -440$ meV are located in tetrahedra with the stoichiometry Ti_3Ni and Ti_2ZrNi throughout the structure. Thus the high-energy sites consist of Ni containing tetrahedra while the low-energy sites have no Ni neighbors indicating the importance of chemistry on the hydrogen site energy. The distribution of energies of sites situated in tetrahedra of the same stoichiometry has a width of about 400 meV, more than half the total width of the hydrogen site energy distribution, demonstrating the importance of geometry for the hydrogen site energy.

The occupation of the hydrogen sites is not a simple filling of the sites according to energies. The two lowest-energy sites H_1 and H_2 show a high-hydrogen occupancy followed by a large number of empty sites. In the following section we discuss how hydrogen-hydrogen interactions modify the hydrogen site energy distribution and prevent the occupation of sites that are closer than about 2 \AA to already occupied sites.

V. HYDROGEN INTERACTIONS

The energy of hydrogen in a metal can be separated into two contributions originating from (1) the interaction between the hydrogen and the metal host atoms and (2) the hydrogen-hydrogen interaction.

A very powerful picture of the hydrogen-metal interaction is provided by the effective medium theory.^{29–31} Using the variational principle of density-functional theory it can be shown³¹ that the binding energy of a hydrogen atom in a solid can be written as $E_{\text{H}}=E_{\text{hom}}(n_0)+E_{\text{corr}}$. The embedding

TABLE II. Hydrogen site energies in the W -TiZrNi phase: The positions of the hydrogen sites are given in order of their energy. For each hydrogen site the experimental occupancy from Table I as well as the number, type, and distance of the nearest metal atom neighbors are listed.

Site	Wyckoff	x	y	z	Tetrahedron	Energy (meV)	Exp. occupancy
H ₁	12(d)	0.000	0.000	0.402	1.92(2Ti), 2.14(2Zr)	-867	0.81
H ₂	48(h)	0.115	0.308	0.191	1.83(2Ti), 1.99(2Zr)	-828	0.68
H ₃	24(g)	0.065	0.000	0.438	1.85(2Ti), 1.99, 2.05(2Zr)	-787	0.00
H ₄	48(h)	0.102	0.072	0.426	1.84(2Ti), 1.98(2Zr)	-678	0.01
H ₅	24(g)	0.000	0.378	0.384	1.80(3Ti), 1.96(Zr)	-671	0.00
H ₆	12(d)	0.000	0.000	0.240	1.81(2Ti), 1.93(2Zr)	-644	0.01
H ₇	24(g)	0.070	0.000	0.183	1.79(3Ti), 1.92(Zr)	-636	0.00
H ₈	48(h)	0.120	0.072	0.194	1.81(2Ti), 1.94(2Zr)	-619	0.00
H ₉	48(h)	0.097	0.136	0.282	1.97(Ti), 2.01(2Zr), 1.65(Ni)	-617	0.06
H ₁₀	48(h)	0.077	0.386	0.191	1.77(2Ti), 1.93(2Zr)	-587	0.01
H ₁₁	24(g)	0.000	0.085	0.358	2.03(Ti), 2.18(2Zr), 1.69(Ni)	-565	0.00
H ₁₂	16(f)	0.113	0.113	0.113	1.79(3Ti), 1.91(Zr)	-563	0.00
H ₁₃	24(g)	0.000	0.427	0.308	1.75(3Ti), 1.93(Zr)	-559	0.13
H ₁₄	48(h)	0.065	0.247	0.228	2.02(Ti), 2.04(2Zr), 1.68(Ni)	-547	0.00
H ₁₅	24(g)	0.000	0.079	0.300	1.95(Ti), 2.01(2Zr), 1.64(Ni)	-496	0.00
H ₁₆	48(h)	0.184	0.262	0.306	1.80(2Ti),1.94(2Zr)	-494	0.00
H ₁₇	48(h)	0.038	0.103	0.372	1.92(Ti),2.06(Zr),1.66(Ni)	-488	0.00
H ₁₈	24(g)	0.000	0.372	0.235	1.79(2Ti),1.92(2Zr)	-448	0.00
H ₁₉	48(h)	0.004	0.191	0.420	1.81,2.03(2Ti),1.99(Zr),1.59(Ni)	-380	0.05
H ₂₀	24(g)	0.106	0.040	0.000	1.79(3Ti),1.62(Ni)	-377	0.00
H ₂₁	48(h)	0.102	0.230	0.285	1.84(2Ti),1.94(Zr),1.59(Ni)	-312	0.00
H ₂₂	16(f)	0.065	0.065	0.065	1.80(3Ti),1.61(Ni)	-303	0.00
H ₂₃	24(g)	0.000	0.290	0.364	1.86(2Ti),1.96(Zr),1.60(Ni)	-293	0.00
H ₂₄	24(g)	0.000	0.289	0.253	1.88(2Ti),1.98(Zr),1.59(Ni)	-260	0.00
H ₂₅	48(h)	0.042	0.268	0.378	1.79, 1.87(2Ti), 1.92(Zr), 1.58(Ni)	-190	0.00

energy $E_{\text{hom}}(n_0)$ describes the energy of a hydrogen atom embedded in a homogeneous electron gas of density n_0 , where n_0 is chosen to be equal to the average density in the region occupied by the hydrogen atom. The embedding energy of hydrogen has a minimum for a density of $n_0 \approx 0.01a_0^{-3}$ and increases almost linearly for higher

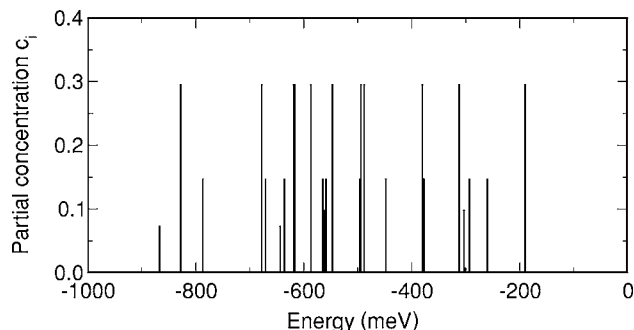


FIG. 3. Density-functional calculations of the hydrogen site energy distribution in the 1/1 approximant structure W -TiZrNi show a broad distribution of sites. A small number of sites around -800 meV is separated from the main distribution ranging from about -700 to -400 meV followed by a tail of sites with higher energy up to -200 meV.

densities.³¹ The increase at higher densities is due to the increase of kinetic energy arising from the repulsion between the hydrogen and the host electrons, whereas the minimum reflects the energy gained when electrons are transferred from the electron gas to the affinity level of the hydrogen atom, corresponding to the electronegativity of the hydrogen atom. The corrections E_{corr} to the binding energy of hydrogen in a solid arise from inhomogeneities of the electron density surrounding the hydrogen atom. They are small when the density distribution is close to the homogeneous electron gas, which usually holds for metals.

Typical electron densities in metals range from 0.02 to $0.08a_0^{-3}$, larger than the density of the minimum in $E_{\text{hom}}(n_0)$. This leads to an almost linear dependence of the embedding energy of hydrogen on the electron density in a metal. The sites of lowest-energy will be the most open sites.

Because the interstitial electron density in most metals is larger than optimum for hydrogen, interstitial hydrogen atoms induce a local expansion of the surrounding lattice. This elastic distortion of the lattice leads to an attractive long-ranged hydrogen-hydrogen interaction, since less work is needed for the lattice expansion for the addition of a second hydrogen atom.^{32,33}

The electron of a hydrogen atom in a metal is delocalized, leading to a proton-screening potential exhibiting a Thomas-

Fermi behavior at short distances and Friedel-type oscillations at large distances.³⁴ The screening charge surrounding the proton induces a repulsive electronic interaction between hydrogen atoms in a metal. This electronic interaction has a short range of about 2 Å in typical metals.¹⁹

Combining the occupation of the hydrogen sites from the Rietveld refinement with the calculated site energies allows us to estimate the minimum distance between hydrogen sites. The hydrogen sites are filled one by one according to energy. The bare energy of the hydrogen sites is modified by the hydrogen-hydrogen interaction. As argued above the dominant hydrogen-hydrogen interaction is repulsive at short distances. The two lowest-energy sites H_1 and H_2 are well separated, with a minimum distance between these sites of 2.8 Å. The high occupancy of these sites indicates that any repulsive interaction at these distances must be weak. Most of the higher-energy sites show a small or zero hydrogen occupation in the Rietveld refinement of Table I. Many of these higher energy sites are within close distance of the sites H_1 and H_2 . Sites H_3 , H_4 , H_8 – H_{11} , H_{14} – H_{18} , H_{21} and H_{24} are within 2 Å of the sites H_1 and H_2 . Of these sites only the sites H_9 shows a small occupation of 0.06. This site is only 1.4 Å from site H_2 , however, site H_2 is only partially occupied by 0.68 hydrogen atoms and hence the distance between hydrogen atoms occupying sites H_2 and H_9 could be larger. The partially occupied sites H_{13} and H_{19} are more than 2.7 Å from sites H_1 and H_2 . The energy difference between the lowest completely empty site and the first site with a significant occupancy, that is site H_{13} with an occupation of 0.13, provides an estimate for the repulsive interaction of about 0.2 eV. Overall these results indicate a repulsive hydrogen-hydrogen interaction with a short range of about 2 Å and a magnitude of roughly 0.2 eV.

To further investigate the short-range electronic interactions between hydrogen atoms¹⁹ we performed a density-functional calculation, placing one hydrogen atom on site H_6 and a second one on site H_{15} with a distance between the two sites of about 1.4 Å. Relaxation of the hydrogen atoms from the initial positions lowers the energy per hydrogen from –88 to –263 meV, while the distance between the hydrogen atoms increases from 1.4 to 2.0 Å. The resulting binding en-

ergy per hydrogen atom of –263 meV is compared to the site energy of an individual hydrogen atom on sites H_6 and site H_{15} of –644 and –496 meV, respectively. This indicates a magnitude of the repulsive interaction of about 0.2 to 0.4 eV, similar to the above estimate. Altogether, the electronic interactions between hydrogen atoms at close range are strongly repulsive and the screening density surrounding a hydrogen atom prevents another hydrogen atom from approaching too close. It also shows that the hydrogen atoms can effectively avoid each other by sitting off center in the interstitial sites. Another effect which can change the energy of the hydrogen sites is the relaxation of the surrounding metal atoms. An estimation of the magnitude of this effect was not attempted here.

VI. CONCLUSION

The locations and energies of hydrogen atoms in the 1/1 approximant structure W -TiZrNi of the icosahedral TiZrNi quasicrystal were determined by a combination of a Rietveld refinement of x-ray and neutron diffraction data and density-functional calculations. About 80% of the hydrogen atoms occupy the two lowest-energy sites. The occupation of the remaining sites is dominated by the short-range repulsive interaction between hydrogen atoms. The range of the repulsive interaction corresponds to the observed closest approach of hydrogen in W -TiZrNi of about 2 Å in good agreement with the work by Switendick.¹⁹ The magnitude of the repulsive interaction is estimated to be 0.2 to 0.4 eV.

ACKNOWLEDGMENTS

The work at Washington University was supported by the National Science Foundation (NSF) under Grants No. DMR 00-72787 and No. DMR 03-07410. R.G.H was partially supported by NSF Grant No. DMR 00-80766 and the Department of Energy Basic Energy Sciences under Grant No. DE-FG02-99ER45795. The authors thank Jay Kim for the preparation of the deuteriated W -TiZrNi sample and Bill Yelon and the Missouri University Research Reactor facility (MURR) for assistance in collecting the neutron spectra.

¹K. F. Kelton, J. J. Hartzell, R. G. Hennig, V. T. Huett, and A. Takasaki, *Philos. Mag.* **86**, 957 (2006).

²R. M. Stroud, A. M. Viano, P. C. Gibbons, K. F. Kelton, and S. T. Mixture, *Appl. Phys. Lett.* **69**, 2998 (1996).

³A. M. Viano, R. M. Stroud, P. C. Gibbons, A. F. McDowell, M. S. Conradi, and K. F. Kelton, *Phys. Rev. B* **51**, 12026 (1995).

⁴E. H. Majzoub, J. Y. Kim, R. G. Hennig, K. F. Kelton, P. C. Gibbons, and W. B. Yelon, *Mater. Sci. Eng., A* **294**, 108 (2000).

⁵M. Bououdina, H. Enoki, and E. Akiba, *J. Alloys Compd.* **281**, 290 (1998).

⁶J. P. Davis, E. H. Majzoub, J. M. Simmons, and K. F. Kelton, *Mater. Sci. Eng., A* **294**, 104 (2000).

⁷R. G. Hennig, E. H. Majzoub, A. E. Carlsson, K. F. Kelton, C. L. Henley, W. B. Yelon, and S. Mixture, *Mater. Sci. Eng., A* **294**, 361 (2000).

⁸R. G. Hennig, K. F. Kelton, A. E. Carlsson, and C. L. Henley, *Phys. Rev. B* **67**, 134202 (2003).

⁹R. G. Hennig, A. E. Carlsson, K. F. Kelton, and C. L. Henley, *Phys. Rev. B* **71**, 144103 (2005).

¹⁰G. Sandroek, National Technical Information Service Report No. ADA328073, Final Report, prepared for Department of the US Navy, Office of Naval Research. Contract N00014-97-M-0001, 1997 (unpublished).

¹¹E. Belin-Ferre, R. G. Hennig, Z. Dankhazi, A. Sadoc, J. Y. Kim, and K. F. Kelton, *J. Alloys Compd.* **342**, 337 (2002).

¹²K. R. Faust, D. W. Pfitsch, N. A. Stojanovich, A. F. McDowell, N. L. Adolphi, E. H. Majzoub, J. Y. Kim, P. C. Gibbons, and K. F. Kelton, *Phys. Rev. B* **62**, 11444 (2000).

¹³R. Feenstra, B. M. Geerken, D. G. deGroot, and R. Griessen, *J. Phys. F: Met. Phys.* **16**, 1965 (1986).

- ¹⁴R. Kirchheim, F. Sommer, and G. Schluckebier, *Acta Metall.* **30**, 1059 (1982).
- ¹⁵A. Szökefalvi-Nagy, S. Filipek, and R. Kirchheim, *J. Phys. Chem. Solids* **48**, 613 (1987).
- ¹⁶F. Jaggy, W. Kieninger, and R. Kirchheim, *Z. Phys. Chem., Neue Folge* **163**, 431 (1989).
- ¹⁷E. Salomons, H. Hemmes, and R. Griessen, *J. Phys.: Condens. Matter* **2**, 817 (1990).
- ¹⁸J. Y. Kim, E. H. Majzoub, P. C. Gibbons, and K. F. Kelton, in *Quasicrystals* edited by J.-M. Dubois, P. A. Thiel, A.-P. Tsai, and K. Urban (Materials Research Society, Warrendale, Pennsylvania, 1999), pp. 483–488.
- ¹⁹A. C. Switendick, *Z. Phys. Chem., Neue Folge* **117**, 89 (1979).
- ²⁰B. K. Rao and P. Jena, *Phys. Rev. B* **31**, 6726 (1985).
- ²¹W. J. Kim, P. C. Gibbons, K. F. Kelton, and W. B. Yelon, *Phys. Rev. B* **58**, 2578 (1998).
- ²²C. L. Henley, *Phys. Rev. B* **43**, 993 (1991).
- ²³A. C. Larson and R. B. von Dreele, Los Alamos National Laboratory Report No. LAUR 86-748 1994 (unpublished).
- ²⁴G. Kresse and J. Hafner, *Phys. Rev. B* **47**, R558 (1993).
- ²⁵G. Kresse and J. Furthmüller, *Phys. Rev. B* **54**, 11169 (1996).
- ²⁶D. Vanderbilt, *Phys. Rev. B* **41**, R7892 (1990).
- ²⁷G. Kresse and J. Hafner, *J. Phys.: Condens. Matter* **6**, 8245 (1994).
- ²⁸J. P. Perdew, in *Electronic Structure of Solids '91* edited by P. Ziesche and H. Eschrig (Akademie Verlag, Berlin, 1991), pp. 11–20.
- ²⁹M. J. Stott and E. Zaremba, *Phys. Rev. B* **22**, 1564 (1980).
- ³⁰J. K. Norskov and N. D. Lang, *Phys. Rev. B* **21**, 2131 (1980).
- ³¹J. K. Norskov, *Phys. Rev. B* **26**, 2875 (1982).
- ³²J. D. Eshelby, *J. Appl. Phys.* **25**, 255 (1954).
- ³³H. Wagner and H. Horner, *Adv. Phys.* **23**, 587 (1974).
- ³⁴H. L. M. Bakker, R. Feenstra, R. Griessen, L. M. Huisman, and W. J. Venema, *Phys. Rev. B* **26**, 5321 (1982).